Enhancement of spontaneous and stimulated emission of a rhodamine 6G dye by an Ag aggregate

M. A. Noginov, G. Zhu, M. Bahoura, C. E. Small, C. Davison, and J. Adegoke
Center for Materials Research, Norfolk State University, Norfolk, Virginia 23504, USA

V. P. Drachev, P. Nyga, and V. M. Shalaev
School of Electrical & Computer Engineering and Birck Nanotechnology Center, Purdue University, West Lafayette, Indiana 47907, USA

(Received 21 February 2006; revised manuscript received 18 July 2006; published 8 November 2006)

We have demonstrated that by adding the solution of aggregated silver nanoparticles to the solution of rhodamine 6G dye, one can enhance the efficiency of spontaneous and stimulated emission. We attribute an increase of the *spontaneous emission* intensity of dye to the increase of the *absorption* efficiency caused by the field enhancements in metallic nanostructures associated with surface plasmons. The enhancement of the *stimulated emission* of dye, which has the same nature as the enhancement of absorption, was observed in the pump-probe and laser experiments.

DOI: 10.1103/PhysRevB.74.184203 PACS number(s): 61.46.Df, 73.20.Mf, 78.67.Bf

I. INTRODUCTION

Localized surface plasmon (SP) is an oscillation of free electrons in metallic nanoparticles, whose resonance frequency is the plasma frequency adjusted by the particles' shape. Localized SPs have been found on rough surfaces,[1,2] in clusters and aggregates of nanoparticles[3–5] as well as in engineered nanostructures.[6–9] In the spots, where local fields are concentrated, both linear and nonlinear optical responses of molecules and atoms are gigantically enhanced. This leads to a number of important applications, the most matured of which is the surface enhanced Raman scattering (SERS).[2] A number of interesting optical phenomena (such as harmonic generation, SERS, Kerr effect, etc.) caused by dramatic field enhancement in hot spots of *fractal aggregates* of silver nanoparticles have been theoretically predicted and experimentally demonstrated by Shalaev *et al.* in Refs. 10–14.

Metallic surfaces and nanoparticles can influence a family of various optical responses. Thus, the dependence of emission spectra and emission lifetimes of luminescent centers on (submicron) distance from a metallic mirror has been discussed in detail in review[15] and references therein. An increase of luminescence intensity of dye molecules *adsorbed* onto islands and films of metal nanoparticles, when the plasma resonances are coupled to the absorption spectra of the molecules, has been observed in the early 80's by Glass *et al.*[16,17] and Ritchie and Burstein.[18] An enhancement and modification of the emission of dye molecules and trivalent rare-earth ions adsorbed onto rough metallic surfaces, metallic islands, engineered structures, etc. have been studied in more recent Refs. 19–23. An increase of optical absorption of CdS quantum dots by gold nanospheres has been demonstrated in Ref. 24.

If a mixture of dye solution and metallic nanoparticles is used as a laser medium, then the SP-induced enhancement of absorption and emission of dye can significantly improve the laser performance. Thus, according to Refs. 25 and 26, in a mixture of rhodamine 6G (R6G) dye with aggregated silver nanoparticles placed in an *optical microcavity* (glass capillary tube), (i) local electromagnetic fields are enhanced by many orders of magnitude, and (ii) the laser action can be obtained at low pumping power, which is not enough to reach the lasing threshold in a pure dye solution of the same concentration.

The experiments in Refs. 25 and 26 were not highly reproducible and the mechanisms of the dramatic reduction of the lasing threshold were not clearly understood at the time. This motivated us to carry out a more systematic study of an analogous system, investigating separately the spontaneous emission, the stimulated emission in a pump-probe setup, and the laser emission in an easy-to-tune two-mirror laser cavity.

II. EXPERIMENTAL SAMPLES AND SETUPS

Experimentally, we studied mixtures of R6G dye (Rhodamine 590 Chloride from Exciton) and aggregated Ag nanoparticles. The starting solutions of R6G in methanol had concentrations of dye molecules in the range $1\times10^{-6}-2.1\times10^{-4}$ M ($6\times10^{14}-1.3\times10^{17}$ cm^{-3}). Poly(vinylpyrrolidone) (PVP) passivated silver aggregate was prepared according to the procedure described in Ref. 27. The estimated diameter of silver nanoparticles was 12 ± 3 nm. The typical network of aggregated silver nanoparicles used in our experiments is shown in Fig. 1. The estimated concentration of Ag nanoparticles in the aggregate was 8.8×10^{13} cm^{-3}. In many measurements Ag was diluted several fold with methanol before mixing it with dye.

Absorption spectra of dye solutions, Ag aggregate solutions, and dye-Ag aggregate mixtures were recorded with the UV-VIZ-IR Lambda 900 spectrophotometer (Perkin Elmer). In the emission measurements, the mixtures of R6G dye and Ag aggregate were excited with the frequency doubled radiation of Q-switched Nd:YAG laser (Quanta Ray, $\lambda=532$ nm, $t_{pulse}=10$ ns). The same pumping was used in the pump-probe gain measurements and the laser experiment. The emission spectra were recorded using MS257 monochromator (Oriel), a photomultiplier tube, and a boxcar integra-

 ©2006 The American Physical Society

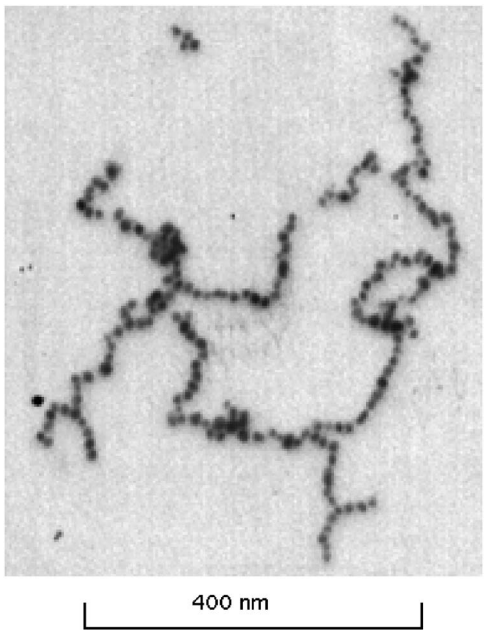

FIG. 1. Transmission electron microscope image of Ag aggregate studied.

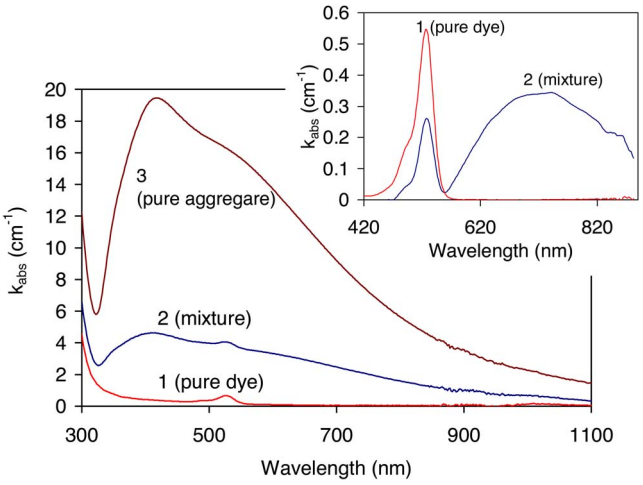

FIG. 2. (Color online) Trace 1—absorption spectrum of the pure R6G dye solution $[2.1\times10^{-6}$ M $(1.3\times10^{15}$ cm$^{-3})]$; trace 3—absorption spectrum of the pure Ag aggregate solution $(8.8\times10^{13}$ cm$^{-3})$; trace 2—absorption spectrum of the Ag aggregate-R6G mixture. The ratio of Ag aggregate solution to R6G solution is equal to 27.1/72.9. Inset. Trace 1—same as trace 1 in the main frame; trace 2—difference absorption spectrum: absorption spectrum of the mixture (trace 2 of the main frame) minus scaled spectrum of the aggregate.

tor. A cw 594 nm He-Ne laser beam was used as a probe in the gain measurements.

In the luminescence kinetics studies, the emission of pure R6G dye solutions and dye-Ag aggregate mixtures was excited with the optical parametric amplifier Topaz (Quantronics/Light Conversion $\lambda=530$ nm, $t_{pulse}=2.5$ ps) pumped with the Spitfire laser system (Spectra Physics). The signal was detected and recorded using 10 GHz GaAs PIN photodetector model ET-4000 (EOTech, rise time <35 ps) and 2.5 GHz oscilloscope TDS7254 (Tektronix).

III. ABSORPTION AND RAYLEIGH SCATTERING MEASUREMENTS

The absorption spectrum of Ag aggregate had one structureless band covering the whole visible range and extending to near-infrared, Fig. 2 trace 3. Note that a fractal aggregate can be roughly thought of as a collection of spheroids, with different aspect ratios and different depolarization factors p, formed by various chains of nanoparticles in the aggregate.[12] Correspondingly, the absorption spectrum of a fractal aggregate is comprised of a continuum of homogeneous bands (having maxima at different wavelengths) corresponding to metallic nanostructures with different effective values of p. The shape of the absorption spectrum of the aggregate, which typically slightly varies from one particular synthesized solution to another, depends on the distribution of the depolarization factors.

The major feature in the absorption spectrum of R6G is the band peaking at ≈528 nm, Fig. 2 trace 1 (main frame and inset). The absorption spectrum of the mixture of Ag aggregate and R6G dye is shown in Fig. 2 trace 2. We scaled the absorption spectrum of pure Ag aggregate to fit the spectrum of the mixture at ≤450 nm and calculated the difference spectrum, inset of Fig. 2 trace 2. The differential spectrum reveals the absorption band of R6G dye and a much broader new absorption band centered at 720–750 nm. This broad band can be due to hybrid states formed by R6G molecules chemisorbed onto silver nanoparticles in the presence of Cl–.[28] The possible effect of chloride ions, known in the literature, includes an increased R6G adsorption caused by the coadsorption with anions, orientation of the adsorbed molecules, and changes in the aggregates structure.[28,29]

Experimentally, we studied Rayleigh scattering by aggregated silver nanoparticles at 558 nm (the wavelength at which R6G dye has practically no absorption) in a variety of samples with different concentrations of Ag aggregate and dye, including pure Ag aggregate suspensions without dye. The experimental setup was similar to that described in Ref. 30, with the only difference that no pumping was used. The intensity of the Rayleigh scattering signal was found to increase linearly (within the experimental accuracy) with the increase of Ag concentration in the suspension and the presence or concentration of R6G dye in the mixture did not matter. This result serves as reasonable evidence that no significant modification of the aggregate occurred due to the presence of dye.

IV. SPONTANEOUS EMISSION

Spontaneous emission spectra were studied in the setup schematically shown in the inset in the upper right corner of Fig. 3(a), when a dye or a mixture of dye with Ag aggregate was placed in a 1 mm cuvette. The sample was pumped and the luminescence was collected nearly normally to the surface of the cuvette. We found that while the shape of the emission band was practically unaffected by the presence of

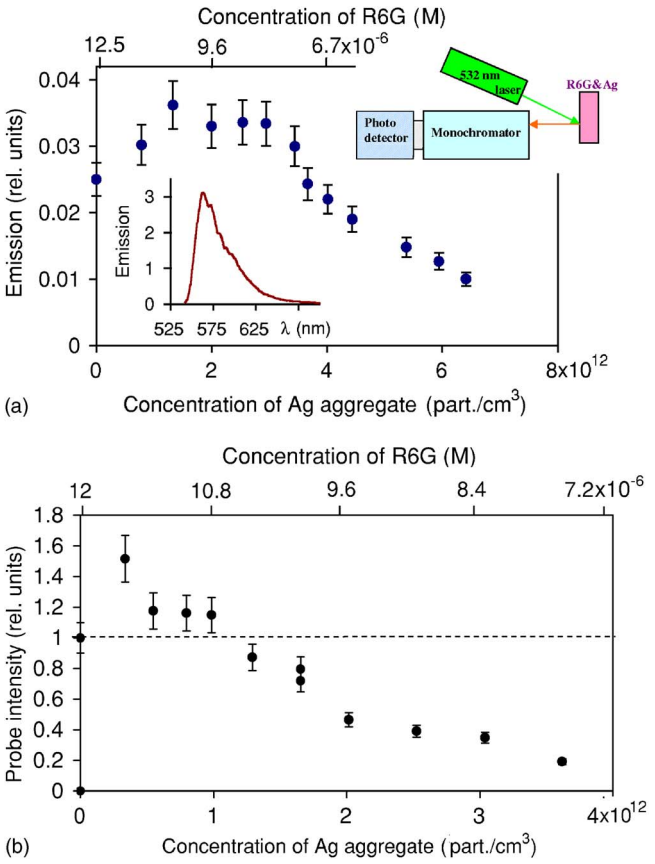

FIG. 3. (a) (Color online) Emission intensity measured at the addition of Ag aggregate to R6G dye. The starting concentrations of R6G and Ag aggregate are, respectively, 1.25×10^{-5} M (7.5×10^{15} cm^{-3}) and 8.7×10^{12} particles/cm^3. The emission intensity corresponds to "as is" detected signal that has not been a subject to any normalization. Inset in the upper right corner: Schematic of the experimental setup used at the emission intensity measurement. Inset in the bottom: Emission spectrum of R6G dye. (b) Probe light intensity (at $\lambda=594$ nm) measured in 10 mm cuvette at the 532 nm pumping energy equal to 0.38 mJ (after 0.5 mm pinhole) as a function of the R6G and Ag aggregate concentrations. All detected signals are normalized to that in pure dye solution.

Ag aggregate in the mixture [inset in the bottom of Fig. 3(a)], its intensity changed significantly. When we started from pure dye solution [1.25×10^{-5} M (7.5×10^{15} cm^{-3})], and added to it in steps small amounts of Ag aggregate (8.7×10^{12} cm^{-3}), diluting dye and increasing the concentration of silver nanoparticles, we observed ~45% increase of the spontaneous emission intensity, Fig. 3(a). [Note that the emission intensity in Fig. 3(a) was not subject to any normalization.]

According to Refs. 31 and 32, the quantum yield of spontaneous emission of low concentrated R6G dye is equal to 95%. Thus, the experimentally observed emission enhancement cannot be due to the increase of the quantum yield. We explain the phenomenon by the increase of the absorption efficiency of R6G dye caused by the field enhancement in the vicinity of metallic nanoparticles. As we discuss in Ref. 30, this increase of the dye absorption is not easy to see in the absorption spectrum of the dye-Ag aggregate mixture

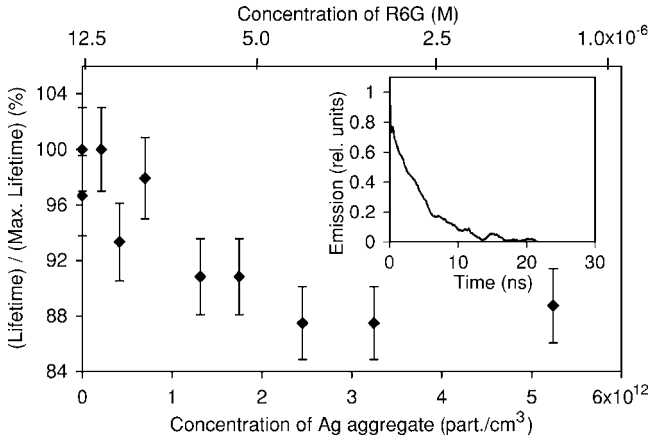

FIG. 4. Dependence of the R6G emission lifetime on concentration of Ag aggregate in dye-Ag aggregate mixtures characterized by low concentrations of R6G dye. All values are normalized to the lifetime measured in the pure R6G solution. Inset: typical emission kinetics.

because dye suppresses the surface plasmon resonance in Ag aggregate and effectively "burns" a hole in its absorption spectrum, which overlaps with the absorption band of the dye.

At the further increase of the concentration of Ag aggregate in the mixture, the emission intensity decreased. This reduction was, in part, due to the absorption by Ag aggregate of both pumping and emission. Another possible reason for the reduction of the emission intensity was quenching of dye luminescence by silver nanoparticles (energy transfer from R6G molecules to silver).

At low concentrations of R6G used in the majority of our experiments, $\leq2.1\times10^{-5}$ M (1.3×10^{16} cm^{-3}), the spontaneous emission kinetics recorded in pure dye solutions were nearly single exponential. The measured time constant was by ~25% larger than the 3.6–3.8 ns lifetime of R6G known from the literature.[33–35] The elongation of the decay kinetics was probably due to the reabsorption, which could not be neglected, since at certain emission wavelengths (~550 nm) the absorption length of dye was comparable to the linear size of the cuvette (~1 cm). When dye [$<2\times10^{-5}$ M (1.2×10^{16} cm^{-3})] was mixed with Ag aggregate ($<1.3\times10^{13}$ cm^{-3}), the effective emission decay time shortened to ~88% of its maximal value in pure dye, Fig. 4. (We assume that the reabsorption was weak enough to affect the qualitative character of the dependence in Fig. 4 significantly.) One can hypothesize that dye molecules, which luminescence decay times are shortened by the presence of Ag aggregate, are situated close to metallic nanoparticles and their absorption and emission properties are affected by SP-enhanced fields.

V. STIMULATED EMISSION STUDIED IN A PUMP-PROBE EXPERIMENT

The enhancement of stimulated emission of R6G dye by Ag aggregate was studied in a pump-probe experiment, which scheme is shown in inset of Fig. 5. The mixture of R6G dye and silver nanoparticles (placed in 10 mm cuvette)

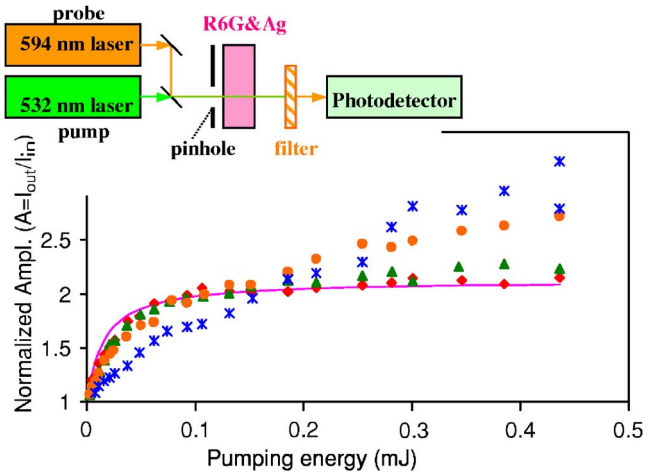

FIG. 5. (Color online) Amplification $A=I_{out}/I_{in}$ (at $\lambda=594$ nm) as a function of the 532 nm pumping energy (after 0.5 mm pinhole) measured in a series of R6G dye-Ag aggregate solutions in 10 mm cuvette. Solid line—calculation corresponding to pure dye, 1.25×10^{-5} M (7.5×10^{15} cm^{-3}). Characters—experiment. Diamonds—pure dye, 1.25×10^{-5} M (7.5×10^{15} cm^{-3}); triangles—dye 1.25×10^{-5} M (7.5×10^{15} cm^{-3}), Ag aggregate—3.6×10^{11} particles/cm^3; circles—dye 9.0×10^{-6} M (5.4×10^{15} cm^{-3}), Ag aggregate—2.5×10^{12} particles/cm^3; crosses—dye 5.1×10^{-6} M (3.1×10^{15} cm^{-3}), Ag aggregate—5.2×10^{12} particles/cm^3. All amplification signals are normalized to the transmission in corresponding not pumped media. Inset: schematic of the experiment.

was pumped with ~10 ns pulses of a frequency-doubled Nd-YAG laser (532 nm) and probed with a cw 594 nm HeNe laser. The two beams were collinear. They were centered at the 0.5 mm pinhole that was attached to the front wall of the cuvette and restricted the diameters of the incoming beams. The amplification of the probe light (during the short pumping pulse) was measured using 1 GHz oscilloscope TDX 784D (Tektronix). To minimize the amount of spontaneous emission light reaching the detector, we used a monochromator, which wavelength was set at 594 nm. To subtract the residual luminescence signal from the amplified probe light, we repeated the same measurements two times, with and without the probe light.

The result of the measurements for a pure R6G dye solution [1.25×10^{-5} M (7.5×10^{15} cm^{-3})] is depicted in Fig. 5 (diamonds). The dependence of the probe light amplification A, defined as the ratio of the output and input probe light intensities I_{out}/I_{in}, on the pumping density $P(t)/S$ can be described by the following equations:

$$0 \approx \frac{dn}{dt} = \frac{P(t)}{Sh\nu_p}\sigma_{abs532}^{\text{dye}}(N-n) - \frac{n}{\tau} \tag{1}$$

and

$$A \equiv \frac{I_{out}}{I_{in}} = \exp(n\sigma_{594}^{\text{dye}}l), \tag{2}$$

where n is the population of the metastable excited state of R6G molecules; N is the total concentration of R6G molecules; $h\nu_p$ is the energy of the pumping photon; τ is the spontaneous emission lifetime; $\sigma_{em594}^{\text{dye}}$ is the emission cross section of R6G at the probe wavelength,[36] $\sigma_{abs532}^{\text{dye}}$ is the absorption cross section of R6G at the pumping wavelength; and l is the length of the cuvette. In the model, we assumed a four-level scheme of R6G,[36] with the pumping transition terminating at a short-lived state above the metastable state. Thus, we neglected any stimulated emission at the *pumping* wavelength. Since the duration of the pumping pulse was twice longer than the luminescence decay time, we assumed a quasi-cw regime of pumping ($dn^*/dt \approx 0$).

A good qualitative and quantitative agreement between the calculation (solid line in Fig. 5) and the experiment (diamonds) confirms the adequacy of the model. The saturation in the system occurs when all dye molecules are excited and stronger pumping cannot cause a larger gain.

When Ag aggregate was added to the mixture, it caused absorption at the wavelength of the probe light. Correspondingly, in order to obtain the true value of A, all measured amplification signals in the dye-Ag aggregate mixtures were normalized to the transmission T of the probe light through the not pumped sample. The transmission of the sample was checked before and after each amplification measurement. In addition, the solution was thoroughly stirred before measuring each new data point. This helped us to minimize the possible effect of the photomodification of the mixture on the measurement results. The analysis of the probe signal kinetics revealed the existence of at least two different photoinduced lenses, both having characteristic times longer than the duration of the pumping pulse, ~10 ns. Those photoinduced lenses did not interfere with the observation (because they developed *after* the amplification measurement was done in 10 ns pulse), and the study of their nature was outside the scope of this work.

The results of the amplification measurements in the mixed samples are summarized in Fig. 5. The most remarkable feature of this experiment is that at the presence of Ag aggregate, the value of the amplification is not limited by the saturation level characteristic of pure dye but grows to larger magnitudes. Since at strong pumping ($\geq$2 mJ) all dye molecules are already excited, the observed enhancement of the amplification cannot be due to the increased absorption efficiency. We speculate that it is rather due to the enhancement of the *stimulated emission* efficiency caused by the field enhancement in the vicinity of aggregated Ag nanoparticles. Note that the enhancement of *stimulated emission* and the enhancement of *absorption* are caused by the same physical mechanisms and are expected to accompany each other.

When we added Ag aggregate to the mixture, we diluted R6G dye. The dilution of dye, on its own, should lead to the reduction of the gain saturation level. Partial absorption of pumping by Ag aggregate should also lead to the reduction of the amplification. These two factors make the result presented in Fig. 5 (enhancement of amplification) even more remarkable.

An increase of the *spontaneous* emission intensity with the addition of Ag aggregate to the mixture is shown in Fig. 3(a). In approximately the same range of the R6G and Ag aggregate concentrations and at very small pumping energies ($\leq$0.4 mJ), we have observed an *absolute* enhancement of the probe light amplification, without any renormalization to

the sample transmission, Fig. 3(b). The observed increase of the amplified signal could be due to the combination of enhancements of stimulated emission and absorption.

It appears likely that the interplay between the enhancements of absorption and emission, which increase an amplified signal, and the dilution of dye as well as an absorption due to Ag aggregate, which reduce amplification, may cause a complex behavior of the system, which is critically dependent on the Ag concentration and pumping intensity.

VI. EFFECT OF AG AGGREGATE ON THE OPERATION OF R6G DYE LASER

The reduction of a lasing threshold in a *glass capillary resonator* with the addition of Ag aggregate to a dye solution has been demonstrated in Refs. 25 and 26. We studied the effect of Ag aggregate on the performance of regular R6G dye laser, the schematic of which is shown in Fig. 6(a). The gain element was 10 mm long cuvette filled with dye or dye-Ag aggregate mixture. It was pumped through a dichroic mirror, which had the reflection coefficient 99.96% at the lasing wavelength $\lambda \sim 558$ nm. In order to approximate the reportedly large quality factor of the resonator used in Refs. 25 and 26, the reflection coefficient of the output mirror was chosen to be very high, 99.7%. Both mirrors were flat. The length of the cavity was 6.8 cm, and the cuvette with the gain medium was positioned approximately in the center of the cavity. The lens with the focal length equal to 18 cm focused pumping light (Q switched 532 nm laser radiation) into approximately 0.5 mm spot in the cuvette. The color filter placed after the output mirror helped to separate the laser emission from the residual pumping leaking through the laser cavity. The constructed laser had reasonably low threshold, was easy to tune and was not highly sensitive to minor misalignments. Thus, it ideally served the purpose of the experiment.

The series of input-output curves corresponding to different concentrations of Ag aggregate in the mixture is shown in Fig. 6(b). With the addition of Ag aggregate to R6G dye, instead of anticipated enhancement of the laser output, we observed an increase of the lasing threshold and a reduction of the slope efficiency. Apparently, at the sets of the parameters, which were used in our experiment, the reduction of the stimulated emission output caused by the dilution of dye and the addition of a gray absorbing substance (Ag aggregate) to the laser cavity overcame the positive effect caused by the surface plasmon field enhancement.

In order to understand the experimental result better, we modeled the lasing threshold in a dye-Ag aggregate laser. We assumed that the concentration of silver nanoparticles in the starting solution of Ag aggregate was equal to $M(\mathrm{cm}^{-3})$ and the concentration of R6G molecules in the starting dye solution was equal to N (cm^{-3}). We also presumed that the mixture had the volume fraction x of Ag aggregate solution and the volume fraction $1-x$ of R6G dye solution. Correspondingly, the concentrations of Ag nanoparticles and dye molecules in the mixture were equal to Mx and $N(1-x)$. As we have shown in Secs. IV and V, the efficiency of absorption and emission of dye molecules is increased in the presence of

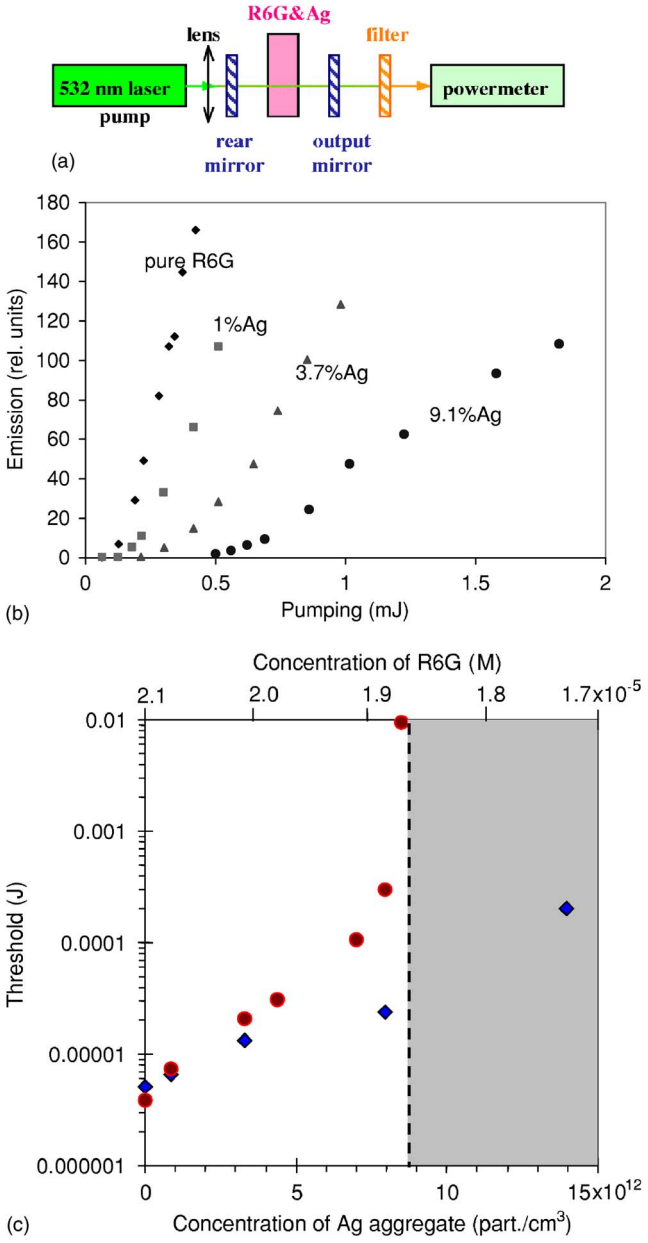

FIG. 6. (a) (Color online) Laser setup. (b) The input-output laser curves (at $\lambda \sim 560$ nm) recorded in a series of samples prepared by mixing small amounts of Ag aggregate (8.8×10^{12} particles/cm^3) with R6G dye [1.1×10^{-5} M (6.6×10^{15} cm^{-3})]. The volume percentage of the Ag aggregate is indicated next to each curve. (c) (Color online) Experimental (diamonds) and calculated (circles) dependences of the laser threshold on Ag aggregate concentration.

Ag aggregate. This increase can be formally treated as an effective enhancement of absorption and emission cross sections. In a first approximation, at $x \ll 1$, the change in the effective cross sections can be described as $\sigma^{\mathrm{dye}}_{em558}(1+a_1x)$, $\sigma^{\mathrm{dye}}_{abs558}(1+a_2x)$, and $\sigma^{\mathrm{Ag}}_{abs532}(1+a_3x)$, where and a_1, a_2, and a_3 are constants and self-explanatory superscripts and subscripts indicate material, wavelength, and emission or absorption. (We assumed that constants a_1, a_2, and a_3 did not depend on the existence or properties of the laser resonator.)

The threshold population inversion n_{th} (cm^{-3}) can be calculated from the formula equating gain and loss in the laser:

$$\exp\{2l\sigma_{em558}^{dye}(1+a_1x)n_{th}\}\exp\{-2l[((N(1-x)-n_{th})\times\sigma_{abs558}^{dye}(1+a_2x))+Mx\sigma_{abs558}^{Ag}]\}R_1R_2(1-L)=1, \quad (3)$$

where l is the length of the laser element, R_1 and R_2 are the reflection coefficients of the laser mirrors, and L is the parasitic intra-cavity loss per round trip caused by the cuvette walls, scattering, etc. Solving this equation for n_{th}, one obtains

$$n_{th}=n_{th}^0\left\{1+x\left[\frac{2lN\sigma_{abs558}^{dye}}{2lN\sigma_{abs558}^{dye}-\ln(R_1R_2(1-L))}\times\left((a_2-1)+\frac{M\sigma_{abs558}^{Ag}}{N\sigma_{abs558}^{dye}}\right)\right]-\frac{\sigma_{em558}^{dye}a_1+\sigma_{abs558}^{dye}a_2}{\sigma_{em558}^{dye}+\sigma_{abs558}^{dye}}\right\}, \quad (4)$$

where

$$n_{th}^0=\frac{2lN\sigma_{abs558}^{dye}-\ln[R_1R_2(1-L)]}{2l(\sigma_{em558}^{dye}+\sigma_{abs558}^{dye})} \quad (5)$$

is the threshold population inversion in the absence of Ag aggregate ($x=0$).

Since the absorption and emission wavelengths are close to each other and the spectral properties of Ag aggregate do not strongly change between 532 nm and 558 nm, one can assume in a first approximation that $a_1=a_2=a_3=a$. If the transmission and scattering loss in the cavity is much greater than the absorption loss at the lasing wavelength, $-\ln[R_1R_2(1-L)]\gg 2lN\sigma_{abs558}^{dye}$, then Eq. (4) can be simplified to a form

$$n_{th}\approx n_{th}^0(1-ax) \quad (6)$$

that suggests a reduction of the threshold population inversion with the increase of Ag aggregate concentration in the mixture. On the other hand, at $-\ln[R_1R_2(1-L)]\ll 2lN\sigma_{abs558}^{dye}$, which is probably close to the conditions of our experiment with highly reflective laser mirrors

$$n_{th}\approx n_{th}^0\left|1+x\left(\frac{M\sigma_{abs558}^{Ag}}{N\sigma_{abs558}^{dye}}-1\right)\right|. \quad (7)$$

Since in our experiment the absorption coefficient of Ag aggregate at the lasing wavelength, $M\sigma_{abs558}^{Ag}$, is much larger than the absorption coefficient of dye, $N\sigma_{abs558}^{dye}$, the threshold population inversion is predicted to increase with the addition of Ag aggregate to the mixture.

The threshold incident pumping energy E_{th} [J] can be calculated from the formula for the threshold rate of pumping absorbed per unit volume F_{th} ($cm^{-3}\ s^{-1}$)

$$F_{th}=\frac{E_{th}}{t_p h\nu_p(Sl)}\{1-\exp[-((N(1-x)-n_{th})\sigma_{abs532}^{dye}(1+a_3x))l]\}\times\left\{\frac{(N(1-x)-n_{th})\sigma_{abs532}^{dye}(1+a_3x)}{[(N(1-x)-n_{th})\sigma_{abs532}^{dye}(1+a_3x)+Mx\sigma_{abs532}^{Ag}]}\right\} \quad (8)$$

which (in the quasi-cw approximation), is related to n_{th} as

$$F_{th}=\frac{n_{th}}{\tau}. \quad (9)$$

Here t_p is the duration of the pumping pulse, τ is the lifetime of the metastable laser level, S is the cross section of the pumping beam, and $h\nu_p$ is the pumping photon energy. In Eq. (8), the first term in figure brackets determines the fraction of incident pumping energy that is absorbed by the sample, and the second term in figure brackets determines the fraction of the total absorbed pumping energy, which is consumed by *dye* (and not by Ag aggregate).

At small value of the threshold population inversion, $n_{th}\ll N$, the effect of Ag aggregate on the threshold energy can be described by the equation

$$E_{th}=E_{th}^0\left|1+x\left(C_1\frac{M\sigma_{abs558}^{Ag}}{N\sigma_{abs558}^{dye}}-C_2a+C_3\right)\right|, \quad (10)$$

where E_{th}^0 is the threshold pumping energy in the absence of Ag aggregate ($x=0$), $a_1=a_2=a_3=a$, and coefficients C_1, C_2, and C_3 depend on the ratio of the transmission and absorption losses at the lasing wavelength as well as optical thickness of the sample at the pumping wavelength. At $M\sigma_{abs558}^{Ag}\gg N\sigma_{abs558}^{dye}$, which corresponds to the conditions of our experiment, the ratio $\frac{M\sigma_{abs558}^{Ag}}{N\sigma_{abs558}^{dye}}$ dominates the expression in the parentheses. Thus, an addition of Ag aggregate to the dye causes an increase of the threshold pumping energy (even at the reduction of the threshold population inversion n_{th}).

The most interesting experimental result is predicted when $-\ln[R_1R_2(1-L)]\gg 2lN\sigma_{abs558}^{dye}$ and the threshold value n_{th} is slightly larger than the total concentration N of R6G molecules in pure dye solution. Obviously, in this case the lasing threshold cannot be achieved at any pumping energy. If with the addition of Ag aggregate, the threshold population inversion will decrease according to formula (6) and become smaller than the total concentration of dye molecules $N(1-x)$, then the lasing will become possible. [The enhancement of spontaneous and stimulated emission depicted in Figs. 3 and 5 suggests that $(1-x)(1+ax)$ is larger than 1 and, correspondingly, $1-x>1-ax$.] Thus, Ag aggregate can enable laser action, which is not possible without Ag aggregate. Silver aggregate can also reduce lasing threshold at large values of n_{th}, which are $\leq N$.

Constants a_1, a_2, and a_3 are not experimentally known. By putting them to be equal to zero, one can calculate the lasing thresholds under the assumption that the only two effects of the Ag aggregate are the dilution of dye and an increase of the parasitic absorption at the pumping and emission wavelengths.

The experimental and the calculated dependences of the laser threshold on the concentration of Ag aggregate are depicted in Fig. 6(c). A good agreement between the experi-

mental and the calculated values of the threshold at the absence of Ag aggregate justifies the accuracy of our model. One can see in Fig. 6(c) that if the enhancements of absorption and stimulated emission by Ag aggregate are neglected and the role of aggregate is reduced to the dilution of dye and the increase of the parasitic absorption, the calculated threshold energies in dye-Ag aggregate mixtures significantly exceed the experimental ones. On the right hand side of the dashed line in Fig. 6(c) no lasing is predicted. In this range of Ag aggregate concentrations, the calculated threshold value of the population inversion exceeds the concentration of dye molecules in the solution.

The data presented in Fig. 6(c) confirm that Ag aggregate enhances the stimulated emission of R6G dye. However, the overall effect of the aggregate on the laser operation is negative.

How one can make the overall effect of Ag aggregate on the laser output to be positive? As it is shown above, a significant reduction of the lasing threshold can be demonstrated at the combination of two conditions: (i) the transmission and scattering loss in the cavity should be much greater than the absorption loss at the lasing wavelength, $-\ln[R_1R_2(1-L)] \gg 2lN\sigma_{abs558}^{dye}$, and (ii) the threshold population inversion is high, comparable to the total concentration of dye molecules in the solution. The experimental demonstration of such lasing regime is the subject of future work.

VII. SUMMARY

To summarize, we have demonstrated that by adding the solution of aggregated silver nanoparticles to the solution of rhodamine 6G laser dye, one can enhance the efficiency of spontaneous and stimulated emission. We attribute an increase of the *spontaneous emission* intensity of dye to the increase of the *absorption* efficiency caused by the field enhancements in metallic nanostructures associated with surface plasmons. The enhancement of the *stimulated emission* of R6G dye, which has the same nature as the enhancement of absorption (SP-induced field enhancement), was observed in the pump-probe and laser experiments. In the dye-Ag aggregate mixtures studied, the positive effect of the stimulated emission enhancement could not overcome the negative effects associated with the dilution of dye by Ag aggregate and parasitic absorption of Ag aggregate.

ACKNOWLEDGMENTS

This work was supported by NASA Grant No. NCC-3-1035 and NSF Grant No. HRD-0317722, NSF-NIRT ECS-0210445, NSF PREM Grant No. DMR-0611430, NSF NCN Grant No. EEC-0228390, and by MURI-ARO Grants No. 50342-PH-MUR and No. 50372-CH-MUR.

[1] R. H. Ritchie, Surf. Sci. **34**, 1 (1973).
[2] M. Moskovits, Rev. Mod. Phys. **57**, 783 (1985).
[3] U. Kreibig and M. Vollmer, *Optical Properties of Metal Clusters* (Springer, New York, 1995), Vol. 25.
[4] K.-H. Su, Q.-H. Wei, X. Zhang, J. J. Mock, D. R. Smith, and S. Schultz, Nano Lett. **3**, 1087 (2003).
[5] M. Quinten, J. Cluster Sci. **10**, 319 (1999).
[6] M. Quinten, A. Leitner, J. R. Krenn, and F. R. Aussenegg, Opt. Lett. **23**, 1331 (1998).
[7] R. D. Averitt, S. L. Westcott, and N. J. Halas, J. Opt. Soc. Am. B **16**, 1824 (1999).
[8] M. L. Brongersma, J. W. Hartman, and H. A. Atwater, Phys. Rev. B **62**, R16356 (2000).
[9] J. J. Mock, M. Barbic, D. R. Smith, D. A. Schultz, and S. Schultz, Chem. Phys. **116**, 6755 (2002).
[10] V. A. Markel, V. M. Shalaev, E. B. Stechel, W. Kim, and R. L. Armstrong, Phys. Rev. B **53**, 2425 (1996).
[11] V. M. Shalaev, E. Y. Poliakov, and V. A. Markel, Phys. Rev. B **53**, 2437 (1996).
[12] V. M. Shalaev, *Nonlinear Optics of Random Media: Fractal Composites and Metal-Dielectric Films, Springer Tracts in Modern Physics* (Springer, Berlin, Heidelberg, 2000), Vol. 158.
[13] *Optical Properties of Random Nanostructures*, edited by V. M. Shalaev (Springer Verlag, Berlin, Heidelberg, 2002), *Topics in Applied Physics*, Vol. 82.
[14] V. M. Shalaev, Phys. Rep. **272**, 61 (1996).
[15] K. H. Drexhage, in *Progress in Optics XII*, edited by E. Wolf (North-Holland, Amsterdam, 1974), p. 164.
[16] A. M. Glass, P. F. Liao, J. G. Bergman, and D. H. Olson, Opt. Lett. **5**, 368 (1980).
[17] A. M. Glass, A. Wokaun, J. P. Heritage, J. G. Bergman, P. F. Liao, and D. H. Olson, Phys. Rev. B **24**, 4906 (1981).
[18] G. Ritchie and E. Burstein, Phys. Rev. B **24**, 4843 (1981).
[19] D. A. Weitz, S. Garoff, J. I. Gersten, and A. Nitzan, J. Chem. Phys. **78**, 5324 (1983).
[20] G. A. Denisenko, G. E. Malashkevich, T. V. Tziganova, V. G. Galstyan, A. P. Voitovich, P. P. Perchukevich, I. I. Kalosha, A. G. Bazilev, B. V. Mchedlishvili, W. Strek, and V. A. Oleinikov, Acta Phys. Pol. A **90**, 121 (1996).
[21] S. T. Selvan, T. Hayakawa, and M. Nogami, J. Phys. Chem. B **103**, 7064 (1999).
[22] J. R. Lakowicz, I. Gryczynski, Y. Shen, J. Malicka, and Z. Gryczynski, Photonics Spectra **35**, 96 (2001).
[23] T. Kikteva, D. Star, Z. Zhao, T. L. Baisley, and G. W. Leach, J. Phys. Chem. B **103**, 1124 (1999).
[24] J. Biteen, I. Garcia-Munoz, N. Lewis, and H. Atwater, California Institute of Technology, Pasadena, California, MRS Fall meeting, 2004.
[25] W. Kim, V. P. Safonov, V. M. Shalaev, and R. L. Armstrong, Phys. Rev. Lett. **82**, 4811 (1999).
[26] V. P. Drachev, W.-T. Kim, V. P. Safonov, V. A. Podolskiy, N. S. Zakovryashin, E. N. Khaliullin, V. M. Shalaev, and R. L. Armstrong, J. Mod. Opt. **49**, 645 (2002).
[27] M. A. Noginov, G. Zhu, C. Davison, A. K. Pradhan, K. Zhang, M. Bahoura, M. Codrington, V. P. Drachev, V. M. Shalaev, and V. F. Zolin, J. Mod. Opt. **52**, 2331 (2005).
[28] P. Hildebrant and M. Stockburger, J. Phys. Chem. **88**, 5935 (1984).

[29] W. Grochala, A. Kudelski, and J. Bukowska, J. Raman Spectrosc. **29**, 681 (1998).
[30] M. A. Noginov, G. Zhu, M. Bahoura, J. Adegoke, C. E. Small, B. A. Ritzo, V. P. Drachev, and V. M. Shalaev, Appl. Phys. B (to be published); M. A. Noginov, G. Zhu, V. M. Shalaev, V. P. Drachev, M. Bahoura, J. Adegoke, C. E. Small, and B. A. Ritzo, physics/0601001 (unpublished).
[31] R. F. Kubin and A. N. Fletcher, J. Lumin. **27**, 455 (1982).
[32] D. Magde, R. Wong, and P. G. Seybold, Photochem. Photobiol. **75**, 327 (2002).
[33] K. A. Selanger, J. Falnes, and T. Sikkeland, J. Phys. Chem. **81**, 1960 (1977).
[34] R. Müller, C. Zander, M. Sauer, M. Deimel, D.-S. Ko, S. Siebert, J. Arden-Jacob, G. Deltau, N. J. Marx, K. H. Drexhage, and J. Wolfrum, Chem. Phys. Lett. **262**, 716 (1996).
[35] C. Zander, M. Sauer, K. H. Drexhage, D.-S. Ko, A. Schulz, J. Wolfrum, L. Brand, C. Eggelin, and C. A. M. Seidel, Appl. Phys. B **63**, 517 (1996).
[36] O. Svelto, *Principles of Lasers*, 4th ed. (Plenum, New York, 1998).